1510–1525 *Nucleic Acids Research, 2011, Vol. 39, No. 4* *Published online 23 October 2010*
doi:10.1093/nar/gkq846

A role for human Dicer in pre-RISC loading of siRNAs

Kumi Sakurai[1,2], Mohammed Amarzguioui[1,3], Dong-Ho Kim[1,4], Jessica Alluin[1], Bret Heale[1,2,5], Min-sun Song[1], Anne Gatignol[6], Mark A. Behlke[7] and John J. Rossi[1,2,*]

[1]Department of Molecular and Cellular Biology, Beckman Research Institute, City of Hope, 1450 East Duarte Road, Duarte, CA 91010, [2]Irell and Manella Graduate School of Biological Sciences, City of Hope, 1450 East Duarte Road, Duarte, CA 91010, USA, [3]The Biotechnology Centre of Oslo, Gaustadalleen 21, 0349 Oslo, Norway, [4]Genolution Pharmaceuticals, Inc. Songpa-gu, Seoul, 138-040, Korea, [5]Human Genetics Unit, MRC, Western General Hospital, Crew Road, Edinburgh Scotland, UK, [6]Virus-cell Interactions Laboratory, Lady Davis Institute for Medical Research, McGill University, Montréal, Canada and [7]Integrated DNA Technologies, Inc. 1710 Commercial Park, Coralville, IA 52241, USA

Received February 27, 2010; Revised August 19, 2010; Accepted September 7, 2010

ABSTRACT

RNA interference is a powerful mechanism for sequence-specific inhibition of gene expression. It is widely known that small interfering RNAs (siRNAs) targeting the same region of a target-messenger RNA can have widely different efficacies. In efforts to better understand the siRNA features that influence knockdown efficiency, we analyzed siRNA interactions with a high-molecular weight complex in whole cell extracts prepared from two different cell lines. Using biochemical tools to study the nature of the complex, our results demonstrate that the primary siRNA-binding protein in the whole cell extracts is Dicer. We find that Dicer is capable of discriminating highly functional versus poorly functional siRNAs by recognizing the presence of 2-nt 3′ overhangs and the thermodynamic properties of 2–4 bp on both ends of effective siRNAs. Our results suggest a role for Dicer in pre-selection of effective siRNAs for handoff to Ago2. This initial selection is reflective of the overall silencing potential of an siRNA.

INTRODUCTION

RNA interference (RNAi) is an evolutionarily conserved process mediated by a multi-component ribonucleoprotein complex called the RNA induced silencing complex (RISC) (1–2). RNAi can be described as having at least two well-defined steps: the initiation step, where the ribonuclease (RNase) III enzyme Dicer processes dsRNAs into 21–22-nt-long duplexes (3), and the effector step, in which Argonaute 2 (Ago 2), a core endonuclease of the RISC, executes RNAi (4–6). Two classes of small regulatory RNAs—small interfering RNAs (siRNAs) and microRNAs (miRNAs)—are shown to associate with RISC as RNAi trigger molecules. SiRNAs, 21–23 nt fully complementary double-stranded RNAs (dsRNAs) with 2-nt 3′ overhangs, guide sequence-specific degradation of complementary messenger RNAs once incorporated into RISC (7–10). In contrast, miRNAs form imperfect duplexes with the target mRNAs, most often in the 3′-UTR, and the miRNA-containing RISC blocks translation or leads to destabilization of the targeted message (11–18).

The RNAse III family member Dicer, along with co-factor RNA-binding proteins, processes long dsRNAs and pre-miRNAs into the functional 21–23-nt siRNA or miRNA duplexes. The functional roles of Dicer have been most well studied in *Drosophila* where two distinct enzymes are involved in parallel pathways for small regulatory RNA biogenesis. Dicer-2 (Dcr-2) processes long-double-stranded precursors and generates siRNAs (19,20) while Dicer-1 (Dcr-1) processes pre-miRNAs into mature miRNAs (20). Importantly, these two enzymes utilize different co-factors for their respective functions. Dcr-1 is associated with the dsRNA-binding protein Loquacious (Loqs) (21,22) whereas Dcr-2 is associated with the dsRNA-binding protein R2D2 (19,23). In contrast, mammals possess only a single species of Dicer in association with the dsRNA-binding protein TRBP, which participates in both si- and miRNA biogenesis (24,25). Given this fundamental difference between human and fly RNAi pathways, we sought to characterize the mechanism by which highly functional siRNAs are selected in humans.

*To whom correspondence should be addressed. Tel: +1 626 301 8360; Fax: +1 626 301 8271; Email: jrossi@coh.org

In humans, the HIV-1 TAR RNA-binding protein (TRBP) has been characterized as one of the factors that assemble Dicer-generated small RNAs into RISC by interacting directly with Dicer and Ago2 (26–29). TRBP has been shown to have versatile roles in small regulatory RNA biogenesis. TRBP has high-sequence similarity to *Drosophila* Loqs and mammalian PACT (30), and is required for both si- and miRNA silencing (27,29). The Dicer-TRBP interaction is RNA independent (29). TRBP is required for the recruitment of Ago2 to the siRNA–Dicer complex (27) and is proposed to participate in coupling of the RNAi initiation and effector steps. Other studies have shown that MOV10 (31,32) and RNA Helicase A (33) are additional factors that associate with human RISC, forming an active complex. However, little is known about their modes of action in RNAi.

The selection of the guide strand which serves as a sequence-specific RNAi trigger largely determines the efficacy of RNAi (3). Effective siRNAs most often have a thermodynamically unstable 5′ guide strand end (34), and often have asymmetric loading of the guide versus passenger strands (35). In *Drosophila*, the orientation of the guide strand of the siRNA is determined by the Dcr-2/R2D2 heterodimer siRNA binding, with Dcr-2 binding at the 5′-end of the guide strand and R2D2 binding the 5′-end of the passenger strand (36). R2D2 is also sensitive to the 5′-end stability and the presence of 5′ phosphates on the siRNA (36).

In comparison to observations with the siRNAs, which often show a wide range of potency (37–39), Dicer processing of its substrates during the initiation step of RNAi was shown to result in better programming of RISC (9,19,28). Furthermore the polarity of Dicer processing preferentially defines which strand serves as the guide (40). Conversely, it is known that Dicer processing is dispensable for RISC assembly and siRNA-mediated cleavage of target-RNA transcripts when siRNAs were exogenously introduced into cells lacking functional Dicer (41–43). Interestingly, in *Drosphila*, an organism which expresses both siRNAs and miRNAs as regulatory small RNAs, the Dcr-2/R2D2 heterodimer was shown to act as a gatekeeper promoting the incorporation of siRNAs for assembly with Ago2 while disfavoring miRNAs as loading substrates for Ago2 (44). The sorting process depends upon the structure of the small RNA duplex and not upon Dcr-2 cleavage.

Aside from the appropriate selection of the guide strand for incorporation into RISC, there is the concern of off-targeting in which either the sense or antisense strand binds to non-targeted sequences triggering inhibition of expression of these transcripts (45–48). Therefore in order to enhance the efficacy of RNAi, it is essential to better understand the mechanism of siRNA selection and strand incorporation in the RNA-silencing pathway.

Here we show that siRNAs associate with a high-molecular weight complex in HEK293 and HCT116 whole cell extracts. The degree of this association varies from siRNA to siRNA, in some cases dramatically between two siRNAs differing by only a single base pair. We observe that Dicer is the core siRNA-duplex-binding component of the whole cell extract complex. Dicer preferentially recognizes the 2-nt 3′ overhangs and thermodynamically unstable ends. Since Dicer can bind to a siRNA duplex in either orientation, either strand of the duplex can be selected as the guide strand based on the thermodynamic end properties of the duplex. Thus, when siRNAs are delivered exogenously to cells, human Dicer (most likely in the form of a complex with TRBP and Ago2) serves as the primary sensor for the selection of highly functional siRNAs leading to handoff to Ago2. This selective process is based upon the presence of ribose 2-nt 3′ overhangs and the thermodynamic end properties of the siRNAs. When siRNAs cannot interact with Dicer, such as in Dicer null cells, they can bypass the Dicer-binding step and directly enter RISC. Nevertheless when Dicer is present, it serves as a primary sensor for siRNA selection when the siRNAs contain an appropriate structure.

MATERIALS AND METHODS

Synthetic siRNAs

All siRNAs used in this study were synthesized by IDT (Coralville, Iowa). The siRNAs were purified using high-performance liquid chromatography. The sequences are listed in Figures 1 and 3.

Cell extracts

HEK293 cells were grown to confluency in 10-cm dishes, harvested and washed with 1x PBS. The cell pellet was re-suspended in 0.5 ml of buffer D (20 mM HEPES, pH. 7.9, 0.2 mM EDTA, 0.5 mM DTT, 50 mM KCl, 10% Glycerol, 0.2 mM PMSF) and sonicated three times for 20 s on ice with a Sonifier 450 (Branson, Danbury, CT) at a setting of 60. The supernatants were collected after 15 min of microcentrifugation for direct use in subsequent experiments.

Dual luciferase reporter assays

To generate reporter plasmids psi-hnRNPH-S (sense reporter) and psi-hnRNPH-AS (antisense reporter), a 343-bp PCR fragment of hnRNPH cDNA (Acc.: NM_005520) was cloned in the 3′-UTR of the humanized *Renilla* luciferase gene in the psiCHECK^{TM}-2 vector (Promega) in either the sense or antisense orientation (40). HCT116 cells at 60–80% confluence in 24-well plates were transfected in duplicate or triplicate with 100 ng of reporter DNA, 25–200 pM siRNA and 0.5 µl Lipofectamine2000 per well, in a total transfection volume of 500 µl. Cells transfected with an irrelevant siRNA were used as mock controls, and an average was calculated from the replicates to set *Renilla*/Firefly luciferase expression to 100%.

For EGFP repression, psi-EGFPS1-S (sense reporter) or psi-EGFPS1-AS was generated by cloning a 245-bp PCR fragment of EGFP in either the sense or antisense orientation in the 3′-UTR of the psiCHECK^{TM}-2 vector (Promega) (40). Forty nanograms of reporter DNA, 20 or 200 pM siRNA and 0.5 µl Lipofectaimine2000 per well were used to transfect HEK293 cells in duplicate at

60–80% confluency in 48-well plates, in a total transfection volume of 200 µl. HEK293 cell lysates were collected 24-h post-transfection and subjected to Dual Luciferase assays (Promega). Transfection was done in duplicate and repeated at least three times. *Renilla* luciferase expression was normalized to internal control Firefly luciferase expression. Cells transfected with an irrelevant siRNA were used as mock controls, and an average was calculated from the replicates to set *Renilla*/Firefly luciferase expression to 100%.

For siDicer, siAgo2 or siTRBP treatment, HEK293 cells were seeded on 10-cm dishes and transfected with 40-nM siRNA-targeting Dicer, Ago2 or TRBP. The sequences of the siRNAs used in this study are as follows: Dicer, 5′-UUUGUUGCGAGGCUGAUU CdTdT-3′; Ago2, 5′-GCACGGAAGUCCAUCUGA AdTdT-3′; TRBP, 5′-UCUACGAAAUUCAGUAGG AdTdT-3′. Forty-eight hours later, the siRNA treated cells were seeded on either 48-well plates or 6-well plates for Dual Luciferase assays or RT-qPCR, respectively. In the second-round transfection, the same procedure described above was used for Dual Luciferase assays. Either with or without 20-nM siDicer, siAgo2 or siTRBP in the second round of transfection produced the same results.

IC_{50} measurements

To generate 50% inhibitory concentration (IC_{50}) curves, HEK293 or HCT116 cells at 60–80% confluency in 48-well plates were transfected in duplicate with 40 ng of reporter DNA (either psiEGFPS1-S or –AS with HEK293 cells and psi-H1-S or –AS with HCT116 cells), siRNAs ranging from 0.2 pM to 15 nM in serial dilutions (a minimal of 10 points measurements) and 0.5 µl Lipofectaimine2000 per well in a total transfection volume of 200 µl. Cell lysates were collected 24-h post-transfection and subjected to the Dual-Luciferase Reporter Assay System (Promega). For each siRNA, transfection was carried out in duplicate and repeated at least three times. Normalization of *Renilla* luciferase expression to internal control Firefly luciferase expression was as described above. IC_{50} curves were generated with GraphPad Prism version 5.01 using the dose response curve equation: $Y = \text{Bottom} + (\text{Top} - \text{Bottom})/(1 + 10[(\text{LogIC50} - X) \times \text{HillSlope})]$ with variable slope. The 95% confidence intervals of IC_{50} values for siRNAs in this study are listed in Figures 3 and 4.

Recombinant proteins

N-terminally His_{6x}-tagged TRBP2 was expressed from the pET11a (+) vector (Novagen) in the *Escherichia coli* BL21DE3 strain. Following 4-h induction with 0.5 mM IPTG, purification of His_{6x}-TRBP2 was performed with Nickel-Nitrilotriacetic acid (Ni^{2+}-NTA) (the QIA expression system, Qiagen) under denaturing conditions. Efficiency of elution steps was determined with 12% SDS–PAGE/coomassie blue staining. The protein was further purified by dialyzing with a 3500 MWCO dialysis cassette (#66110, PIERCE, Rockford, IL), concentrated with an Amicon Ultra centrifugal filter 30KNMWL and stored in buffer D containing 10 mM TCEP. Purity of His-TRBP was also determined by Coomassie blue staining and western-blot analyses (49) with an α-His tag antibody (ab18184, Abcam Inc., Cambidge, MA). Recombinant human Dicer was purchased from Ambion, and its concentration was determined with A_{205} measurements. Titration-binding assays were performed to evaluate optimal concentrations of the recombinant proteins (data not presented), ranging from 0.1 µg to 5 µg for Dicer and 4 ng to 300 ng for TRBP, 2 µg of rDicer enzyme and 80 ng of rTRBP were used in subsequent gel shift assays (Figure 5).

Immunodepletion assays

Immunodepletion analyses were carried out as previously described (49). To immunodeplete Dicer, TRBP or Ago 2 from HEK293 whole cell extracts, 2 mg of pre-cleared extract were incubated with each primary antibody—α-Dicer (15 µg of sc-30226, Santa Cruz Biotechnology, Inc., Santa Cruz, CA), α-TRBP [25 µl of TRBP-JBX, (50)], α-Ago2 (15 µg of ab57113, Abcam Inc., Cambridge, MA). In the case of Dicer/TRBP or Ago2/TRBP double immunodepletion, TRBP precipitation was performed following Dicer or Ago2 precipitations. Pre-immune serum (2.5 µl of sc-2007 or sc-2025, Santa Cruz Biotechnology, Inc.) was used as a control. Following 2-h incubation, protein A/G plus agarose beads (Santa Cruz Biotechnology, Inc.) were added and incubated overnight at 4°C with gentle agitation. The following day, supernatants were collected for additional incubation with the beads for 6 h. After removing the beads by a brief microcentrifugation, buffer D was added to bring the cell extracts to a final concentration of 4 mg/ml. Of total protein extracts, 15 µg were used in the Gel Shift assays. Of the cell extracts, 150 µg were also used in western-blot analyses to evaluate the efficiency of the immunodepletions. Equal amounts of total protein were electrophoresed in SDS–PAGE gels (16 cm × 16 cm), and each protein was detected sequentiqlly. After confirming the reproducibility of the procedure, the membrane was cut in three pieces to detect Dicer (~215 kDa), Ago2 (~100 kDa), TRBP (~40 kDa) and b-actin (~37 kDa), and the whole membrane was scanned at once for consistency using two different wave lengths. Antibodies α-Dicer (ab14601, Abcam Inc.), α-Ago2 (ab57113, Abcam Inc.), α-TRBP (ab42018, Abcam Inc.) or α-β-Actin (A5441, Sigma-Aldrich, St. Louis, MO) were used to detect the corresponding proteins. Additionally, the molecular weights of TRBP and Beta-actin are very close. Thus in order to avoid stripping the membrane between each probing, the secondary antibodies—anti-mouse-800nm (610-132-121, Rockland, Gilbertsville, PA) or anti-rabbit-680nm (A21109, Molecular Probes/Invitrogen)—were detected at two different wavelengths on an Odyssey Infrared imaging system (LI-COR biosciences, NE). Scanned results in green, red or yellow were visualized as black and white. The reproducibility of the immunodepletions was verified four times.

Gel-shift assay

For incubations with radio-labeled siRNAs, single-stranded siRNAs were 5′-end labeled with T4 polynucleotide kinase (New England Biolabs) and γ-^{32}P-ATP (MP Biochemicals) for 1 h and purified with a G25 column (GE Healthcare). For siRNA duplexes, independently radio-labeled sense and antisense strands were mixed and annealed at 95°C in a heat block for 2 min and allowed to cool slowly at room temperature by removing the heat block from the heat source until they reached ambient temperature. SiRNA duplexes that were radiolabeled after annealing yielded identical results. Unlabeled EGFPS1-A, –B, hnRNPH-1 and -3 siRNA duplexes were used as cold competitors. For siRNAs with only one 5′-end-labeled strand, the sense or antisense strand was annealed with the unlabeled complementary strand to generate S*/AS or S/AS* EGFPS1A or unlabeled sense and antisense strands were annealed and used as a cold competitor. Of total protein in buffer D, 15.0 μg were incubated with 1 nM (4×10^4 c.p.m.) of labeled siRNA duplexes for 30 min at room temperature. In competition assays, cold siRNA competitors of concentrations at 2, 5, 10, 25, 50 or 100 nM were incubated in addition to 1 nM of labeled EGFPS1A siRNA duplex. The samples were mixed with 4X native gel loading dye and resolved in a 4.5% non-denaturing polyacrylamide gel (29:1) (20×30 cm glass plates, 1.5 mm spacers) with 1X TBE for 3.0 h at 200V and 4°C. The gel was dried at 80°C for 1 h for autoradiography. Quantifications of the RNA–protein complexes were performed with densitometric scanning of the gel (Typhoon scanner). The percent complex binding was calculated as percent bound [bound/ free+bound) $\times$ 100] of siRNAs relative to input siRNA incubated without the cell extract. Percentage bound of the HEK293 WCE sample was set to 100%, and relative intensities of complexes formed in immunodepleted cell extracts were calculated accordingly.

For the gel supershift assays, HEK293 cell extract (15.0 μg of total protein) was incubated with 1 μg of antibody specific for Dicer (ab14601), Ago1 (07-599, Upstate, Lake Placid, NY), Ago2 (07-590, Upstate) or 1 μl TRBP antibody Ab672 (51) for 15 min prior to the incubation with siRNA duplexes. The samples were resolved in a composite polyacrylamide (3%)–agarose (0.5%) gel and run for 7 h at 100V at 4°C. The gel was fixed with a 10% Acetic Acid: 10% methanol mix for 20 min and dried at 80°C for 1 h for autoradiography. The antibodies used in the supershifts were also used in western blot analyses (49) to detect the proteins in the cell extract. The assays described above were repeated multiple times and representative gel figures are shown in this study.

RT-qPCR

Twenty-four hours after the second round of transfection with 20-nM siRNA-targeting Dicer, Ago2 or TRBP, and 200-pM siEGFPS1A variants, RNA was extracted with RNA STAT60 (TEL-TEST), treated with Turbo DNA-Free Kit (Ambion, Austin, Texas) and reverse-transcribed into complementary DNA (cDNA) using random hexamer primers and Maloney Murine Leukemia Virus (MMLV) reverse transcriptase (Invitrogen, Carlsbad, California). One RNA sample of each preparation was processed without MMLV RT as a negative control in subsequent real time PCR reactions. Quantitative analysis of Dicer, Ago2 and TRBP expressions was performed by real time PCR SYBR Green I (Bio Rad) analysis (C1000 Thermal Cycler, Bio Rad, Hercules, California). Dicer, Ago2 and TRBP expression was detected using 50 ng of cDNA, amplified with corresponding primer sets Dicer-A (5′-CATGGATAGTGGGATGT CAC-3′), Dicer-B (5′-CTACTTCCACAGTGACTC TG-3′); Ago2-A (5′-CGCGTCCGAAGGCTGCTC TA-3′), Ago2-B (5′-TGGCTGTGCCTTGTAAAACGC T-3′) and 5′TRBP (5′-GGGCTGCCTAGTATAGAG C-3′), 3′TRBP-2 (5′-GACCCGGAAGGTGAAATT AG-3′). GAPDH expression was detected as internal control using 50 ng of cDNA, with primers GAPDH-A (5′-CGCTCTCTGCTCCTCCTGTT-3′) and GAPDH-B (5′-CCATGGTGTCTGAGCGATGT-3′). PCR conditions are as follows: (i) Dicer, Ago2 and GAPDH PCR: 95°C for 5 min, followed by 40 cycles of 95°C for 30 s, 60°C for 30 s and 72°C for 1 min, and (ii) for TRBP and GAPDH: 95°C for 5 min, followed by 40 cycles of 95°C for 1 min, 60°C for 1 min and 72°C for 1 min.

RESULTS

Differential whole-cell-extract complex formation and target knockdown correlate with siRNA end structure

To test the structural requirements for binding of siRNAs to components of whole cell extracts and target knockdown, various 3′-end modified versions of a single EGFP-targeting siRNA (EGFPS1) were incubated in whole-cell extracts for evaluation of complex formation and in cell culture for target down-regulation assays. The sequence of the antisense (guide) strand of the EGFPS1A variants was kept constant and only the sense strand was varied to create the differing types of overhangs (Figure 1a). The results of the binding assays revealed that differences in complex formation are sensitive to the 3′-end structure. When the siRNA duplexes in Figure 1a were incubated with a HEK293 whole-cell extract, the strongest binding was observed with the 2-nt 3′ overhang (EGFPS1A or 19 + 2 in Figure 1a and b) and was reduced with subsequent alterations in the siRNA end structure. Binding reached <40% with the 21 + 0 (blunt 3′-end) siRNA and complex formation and was further reduced with 5′ overhangs (20-1 or 19-2 in Figure 1a and b), indicating that the complex is formed preferentially with siRNAs via the 3′ overhangs, consistent with binding being initiated with siRNA 3′ overhang-PAZ domain interactions.

To determine whether the 3′-end modifications introduced in the EGFPS1A variants affect RNAi efficacy, the above siRNA variants were tested in the Dual Luciferase reporter assays (Figure 1c). Silencing efficiency for many siRNAs is known to be concentration dependent. Since a high concentration of a given siRNA in an experimental setting could result in masking the

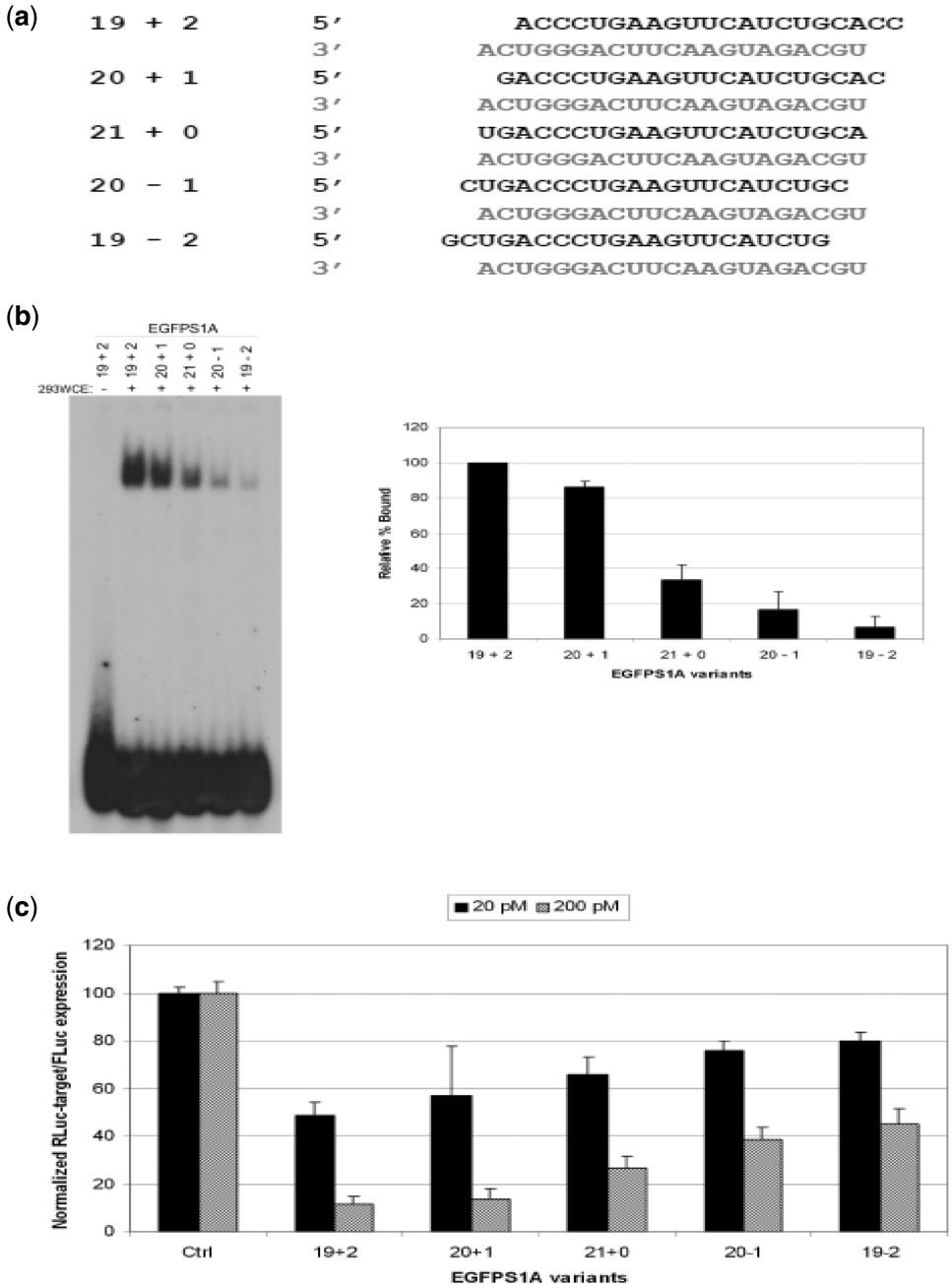

Figure 1. The effect of 3′ overhang on complex formation and RISC function. (a and b) Four variants of EGFPS1A siRNA differing in the number of nucleotides at 3′-end (a) were evaluated for complex formation competence (b) + 2, + 1, + 0, − 1, −2 indicate numbers of nucleotides at the 3′-end as overhangs [19 + 2, 20 + 1, 21 + 0 (blunt ends), 20 – 1 (with 1-nt 5′ overhangs) and 19 – 2 (with 2-nt 5′ overhangs)]. The bottom strands are the antisense sequences and the upper strands the sense sequences. Without HEK293 whole-cell extract, 19 + 2 was included as a negative control. The band shifts were quantified by densitometric scanning of the gel (Typhoon scanner) and percent bound siRNAs were calculated by [bound/(free + bound) × 100] of siRNAs relative to input siRNA without cell-extract incubation. The assays were conducted multiple times with similar results, and a representative gel is shown here. (**c**) Dual Luciferase assays. To determine the efficiency of the 3′-end modified siRNAs in intracellular target knockdown efficiency, silencing by the antisense strand of the end modified EGFPS1A siRNA duplexes was assayed in HEK293 cells by co-transfecting the psi-EGFP-S1 sense reporter and 20- or 200-pM siRNAs. Target-specific *Renilla* luciferase expression was normalized to the control Firefly luciferase expression for all replicates (determined from multiple co-transfections).

effects of various structural features, we chose to use concentrations of 20 and 200 pM, or a concentration at the EGFPS1A IC50 value (Figure 3) versus one 10-fold above this. The variant siRNAs were co-transfected with the psiEGFPS1-S reporter plasmid in HEK293 cells and the effects on *Renilla* luciferase activity were monitored. The 19 + 2 siRNA was most potent, consistent with it being the best binder in the extracts. The other siRNAs followed in graded fashion with the + 1, blunt, −1 and −2 siRNAs being progressively worse in target knockdown. These

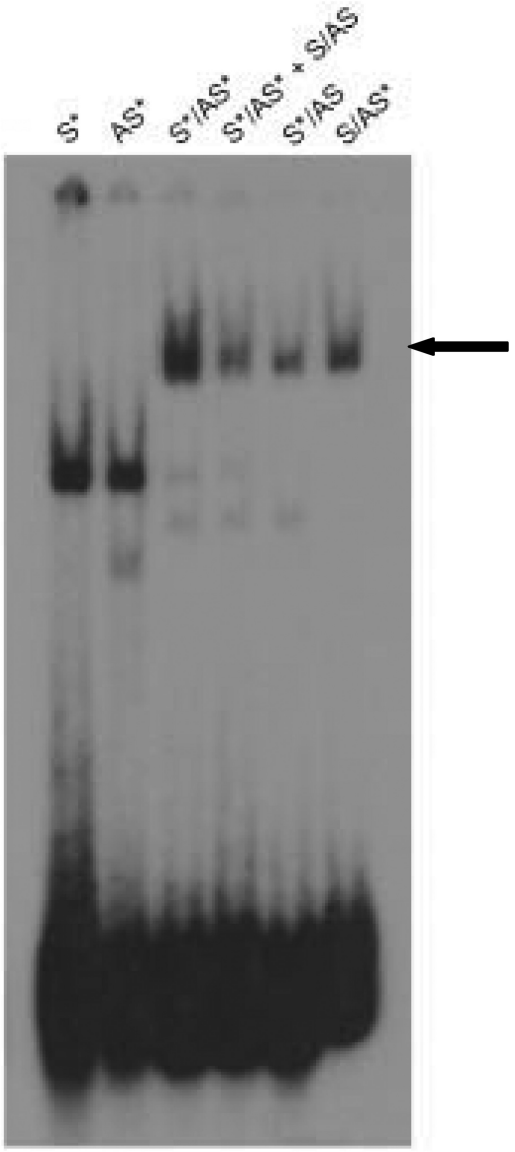

Figure 2. Duplex specificity of siRNAs for complex formation. (A) Duplex requirement for complex formation. Sense (S*) or antisense (AS*) strand of EGFPS1A siRNA was incubated separately in the cell extract, and their gel shift patterns were compared with the intact EGFPS1A duplex. The duplex specificity of the complex was further tested with EGFPS1 A siRNA containing either one (S*/AS or S/AS*) or both (S*/AS*) 5′-labeled strands (lanes 3–6). Cold S/AS was added as a competitor (lane 4). Both S*/AS and S/AS* EGFPS1A were incorporated into the complex (arrow).

cellular assays were consistent with their binding activities in the cell extracts.

We next tested the specificity of complex formation with single- or double-stranded siRNAs to determine if the high-molecular weight complex observed is an RNA duplex specific (Figure 2). When either the EGFPS1A labeled sense (S*) or antisense (AS*) strands were tested individually in the binding assays, no binding to the high-molecular weight complex was observed (Figure 2) whereas a faster migrating complex was observed with both of the single-strand RNAs. We further tested the duplex requirement of the complex using EGFPS1A containing either one (S*/AS or S/AS*) or both (S*/AS*) 5′-radiolabeled strands. Both S*/AS and S/AS* were incorporated into the complex, and cold EGFPS1A (S/AS) efficiently competed with the S*/AS* siRNA–protein complex, confirming that the complex in this study is duplex specific (Figure 2a). These observations demonstrate that the complex formation in this study is preferentially with the duplex form of siRNAs. Our observations are also consistent with reported observations that the human RLC forms exclusively with the duplex form of siRNAs (27–29).

To test the complex formation with several different canonical siRNAs harboring 19-base duplexes and 2-nt overhangs, we created a set of ten siRNAs targeting EGFP (EGFPS1-A–J, Figure 3a) in which each sequence is shifted by 1 nt towards the 5′-end of the target RNA. Several, but not all of the siRNAs incorporated published siRNA features that contribute to the overall efficiency of RNAi (such as an A at position 3 or 19 and 30–50% overall GC content in the passenger strand) (37,39,52–54). Duplex end free energies—from 2 to 5 bp on both the 5′- and 3′-ends—of the siRNAs were also calculated and are listed in Table 1, panel a. When the 10 ^{32}P-labeled anti-EGFP siRNA duplexes were incubated in HEK293 cell extracts and subjected to EMSA analyses, the duplexes formed complexes that migrated similarly. However, while the majority of siRNAs formed strong complexes, EGFPS1B, I and J formed weak complexes (Figure 3b). We next examined the relative levels of siRNA-directed mRNA knockdown using Dual Luciferase assays. IC_{50} values for both sense (S) and antisense (AS) targets of the siRNAs were determined using dose-dependent target knockdown measurements (Figure 3c and Supplementary Figure S1). When the EGFPS1 siRNAs were co-transfected with *Renilla* luciferase target reporter plasmids—psiEGFPS1-S or psiEGFPS1-AS (40)—into HEK293 cells, differential knockdown efficiencies of the siRNAs were observed (Figure 3c). The general trend observed was that the siRNAs with the stronger complex formation percentages (Figure 3b) had better overall combined IC50 values (Figure 3c). In contrast, the three siRNAs with the poorest complex formation percentages (EFGPS1B, I and J, Figure 4b) had high-combined IC50 values (Figure 3c), and in the case of S1J there was no measureable target knockdown for the psi-EGFPS1-AS target (Figure 3c).

As representatives of good and poor binders in the HEK293 cell extract assay, EGFPS1A and B were subsequently incubated with HCT116 cell extracts. Consistent with the observation from the HEK293 cell extract, EGFPS1A and B formed strong and weak complexes, respectively, in the HCT116 cell extract (data not shown), validating that the siRNA-binding differentials are not extract dependent.

To further explore the relationship between complex formation in the whole-cell extracts and RNAi efficacy, we created an additional set of siRNAs targeting a human gene encoding the heterogeneous nuclear ribonucleoprotein (hnRNP) H and tested these for

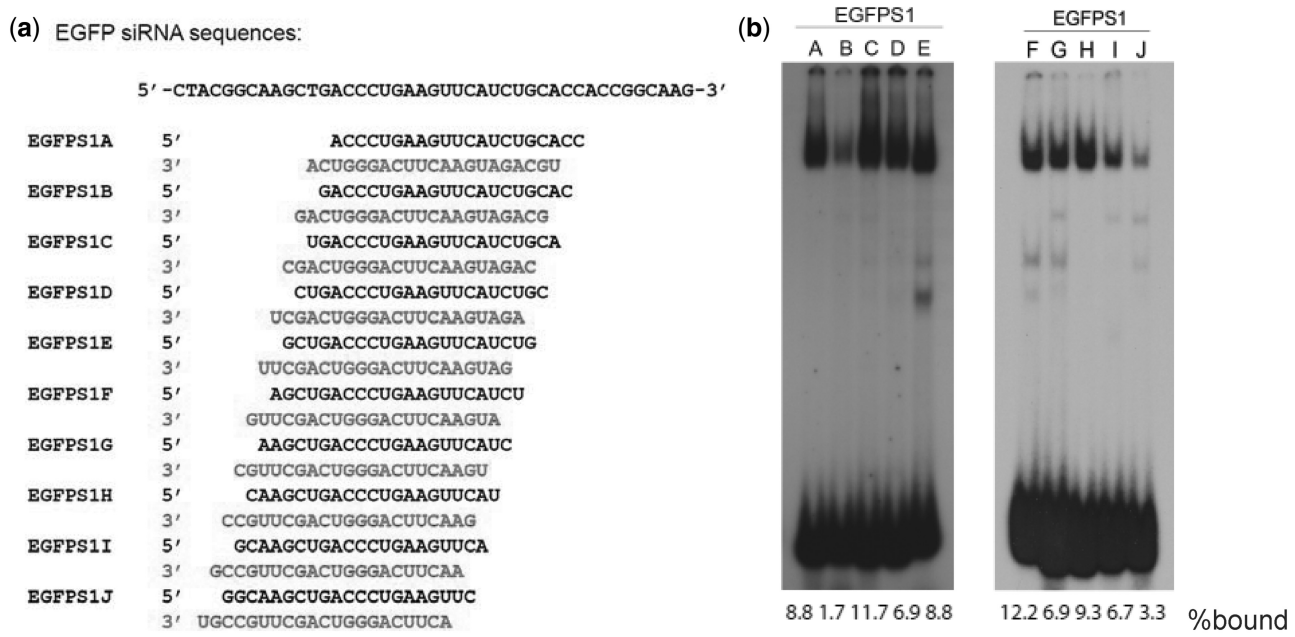

(c) EGFPS1 siRNA IC_{50} values (pM)

Targets:	psi-EGFPS1-S		psi-EGFPS1-AS	
	IC_{50} (pM)	95% confidence interval	IC_{50} (pM)	95% confidence interval
S1A	18.5	16.6 to 20.8	17.6	13.1 to 23.6
S1B	50.4	41.3 to 61.7	80.4	56.0 to 116
S1C	11.4	9.65 to 13.4	16.0	12.9 to 19.7
S1D	11.2	9.90 to 12.7	14.4	11.4 to 18.1
S1E	18.2	15.8 to 21.0	186	47.3 to 730
S1F	9.31	8.27 to 10.5	39.0	30.8 to 49.3
S1G	5.69	5.11 to 6.33	54.8	29.4 to 102
S1H	63.0	44.3 to 89.4	65.7	39.2 to 110
S1I	13.1	9.05 to 19.1	449	0.971 to 208000
S1J	13.3	9.22 to 19.1	n.a.	n.a.

Figure 3. Ribonucleoprotein complex formation and EGFPS1 siRNA silencing. (**a**) A set of 10 anti-EGFP siRNAs-targeting EGFP Site I (40). Upper strand is sense; bottom strand is antisense. (**b**) Gel-shift assays. Anti-EGFPS1-A to -J siRNAs were incubated with HEK293 cell extract and resolved in a 4.5% non-denaturing gel. The band shifts were quantified as described in Figure 1. The assays were conducted multiple times with similar results, and a representative gel is shown here. (**c**) Determination of EGFPS1 siRNA IC50 values. HEK293 cells were co-transfected with either psiEGFPS1-Sense or -Antisense reporter plasmid and an siRNA ranging from 0.2 pM to 1.5 nM in serial dilutions (a minimal of 10 points measurements). Cell lysates collected 24-h post-transfection was subjected to the Dual-Luciferase Reporter Assay System (Promega) (dose-dependent target knockdown measurement curves are shown in Supplementary Figure S1). The n.a. indicates knockdown data were not obtainable for the passenger strand of S1J.

complex formation in HCT116 whole cell extracts (Figure 4). Seven 21-nt-long siRNAs (hnRNP H1–7) were designed with their sequences shifted 1 nt toward the 3′-end of the target RNA hnRNP H (Figure 5a) (40) and these were evaluated in the extracts by EMSA. As with the first set of siRNAs, duplex end-free energies—from 2 to 5 bp on both the 5′- and 3′-ends—of the siRNAs were also calculated and are listed in Table 1, panel b. When the seven ^{32}P-labeled anti-hnRNPH siRNA duplexes were incubated in HCT116 cell extracts and subjected to EMSA analyses, the duplexes formed complexes that migrated similarly (Figure 4b). However, among the seven anti-hnRNP H siRNAs, which were shifted by a single base from each other, we observed a range of binding efficiencies: hnRNP H1, H2, H4 and H7 were effectively incorporated into the complex, whereas

Table 1. Duplex end-free energy calculations (kJ/mol)

siRNA	5′-duplex end				3′-duplex end				Sum of duplex ends			
	2 bp	3 bp	4 bp	5 bp	2 bp	3 bp	4 bp	5 bp	2 bp	3 bp	4 bp	5 bp
Panel a												
S1A	−1.8	−5.1	−8.4	−10.5	−2.1	−5.5	−7.6	−9.7	−3.9	−10.6	−16	−20.2
S1B	−4.6	−6.8	−10.1	−13.4	**−5.6**	**−7.7**	**−9.8**	**− 12.2**	−10.2	−14.5	−19.9	−25.6
S1C	−2.9	−5.3	−7.5	−10.8	−2.5	−4.6	−7	−8.1	−5.4	−9.9	−14.5	−18.9
S1D	−2.5	−4.6	−7	−9.2	−2.8	−5.2	−6.3	−8.4	−5.3	−9.8	−13.3	−17.6
S1E	−4.6	−6.7	−8.8	−11.2	−3.6	−4.7	−6.8	−9.2	−8.2	−11.4	−15.6	−20.4
S1F	−1.7	−5.1	−7.2	−9.3	−0.7	−2.8	−5.2	−6.1	−2.4	−7.9	−12.4	−15.4
S1G	−1.6	−3.7	−7.1	−9.2	−2.2	−4.6	−5.5	−7.7	−3.8	−8.3	−12.6	−16.9
S1H	−2.5	−3.4	−5.5	−8.9	−4.6	−5.5	−7.7	−9.8	−7.1	−8.9	−13.2	−18.7
S1I	−4.2	−6.3	−7.2	−9.3	−0.5	−2.7	−4.8	−5.7	−4.7	−9	−12	−15
S1J	**−5.5**	**−8.9**	**−11**	**−11.9**	−1.8	−3.9	−4.8	−7.2	−7.3	−12.8	−15.8	−19.1
Panel b												
H-1	−0.5	−2.7	−4.8	−5.7	−2.7	−4.8	−5.9	−8.3	−3.2	−7.5	−10.7	−14
H-2	−1.8	−3.9	−4.8	−6.9	−1.7	−4.1	−6.2	−7.3	−3.5	−8	−11	−14.2
H-3	−2.7	−3.6	−5.7	−8.1	−2.7	−3.6	−6	−8.1	−5.4	−7.2	−11.7	−16.2
H-4	−1.7	−3.8	−6.2	−7.1	−1.8	−3.9	−4.8	−7.2	−3.5	−7.7	−11	−14.3
H-5	−2.4	−4.8	−5.7	−6.8	**−4.6**	**−6.8**	−8.9	−9.8	**−7**	**−11.6**	−14.6	−16.6
H-6	**−4.6**	**−5.5**	**−6.6**	−9	−2.4	−4.8	−7	−9.1	**−7**	**−10.3**	−13.6	−18.1
H-7	−0.5	−1.6	−4	−6.1	−1.7	−3.8	−6.2	−8.4	−2.2	−5.4	−10.2	−14.5

Boxes in gray represent thermodynamically more stable ends and numbers in bold face represent the most stable free-energy values among the siRNAs tested in each group.

hnRNPH3, H5 and H6 were poorly incorporated (Figure 4b).

To determine the target knockdown efficacies of the siRNAs in intact cells the relative levels of target inhibition in HCT116 cells was evaluated using Dual Luciferase assays. The reporter system contained an hnRNPH PCR fragment in either a sense (psi-H1-S) or antisense (psi-H1-AS) orientation in the 3′-UTR of a *Renilla* luciferase reporter gene (40). The individual siRNAs were co-transfected with the sense or antisense oriented target plasmids and IC50 values were determined for both siRNA strands (Figure 4c and Supplementary Figure S2). The three siRNAs that showed poor complex formation (H3, H5 and H6) had one or both strands with high-IC50 values, whereas those that had stronger complex interactions (H1, H2, H4 and H7) had overall lower combined S/AS IC50 values (Figure 4c).

The differential strength of complex formation between EGFPS1A versus EGFPS1B and hnRNPH1 versus hnRNPH3 were examined in greater detail using cold siRNAs as competitors for complex formation (Figure 5). Using EGFPS1A as a radio-labeled ligand, unlabeled EGFPS1A, EGFPS1B, hnRNPH1 or hnRNPH3 at 1:2 to 1:100 molar excess were incubated in the HEK293 cell extracts. When hnRNPH1 ($IC_{50S\ and\ AS}$ = 9.03 and 5.04 pM, Figure 4c) was incubated with EGFPS1A ($IC_{50S\ and\ AS}$ = 18.5 and 17.6 pM, Figure 3c), it competed effectively throughout the range of concentrations tested, while EGFPS1B ($IC_{50S\ and\ AS}$ = 50.4 and 80.4 pM, Figure 3c) was a weak competitor. HnRNPH3 ($IC_{50S/AS}$ = 29.7 and 7.66 pM, Figure 4c) was moderately competitive with EGFPS1A for complex formation. These results demonstrate that siRNAs with good potency in cells are good competitors for complex formation in cell extracts, and vice versa, implicating selective siRNA incorporation takes place in the RISC-loading complex (RLC) as well as in RISC itself.

Examination of the roles Dicer, TRBP and Ago2 in complex formation

The results described above were carried out using either the HEK293 or HCT116 cell lines. In order to further explore the complex composition, we carried out additional biochemical experiments in the HEK293 cell extracts. The human RLC consists of Ago2, Dicer and TRBP (26–29). To determine whether any of these components are involved in the siRNA-complex binding observed in this study, we carried out antibody-mediated super-shift assays with HEK293 cell extracts using antibodies against Dicer, TRBP, Ago2 (and Ago1) to monitor complex formation with the EGFPS1A and hnRNPH1 siRNAs (Figure 6). Addition of the anti-Dicer antibody resulted in a strong super-shift of the complex whereas the anti-TRBP antibody yielded a weak but reproducible supershift. These results indicate that the complex observed in Figures 1–3 contain at least Dicer and TRBP, consistent with the previous observation by Pellino et al. (55). Although no supershifts were observed with the anti-Ago2 or anti-Ago1 antibodies, these antibodies did recognize the cognate proteins in the HEK293 whole cell extract (Figure 6).

To further analyze the complex components, Dicer, TRBP, Dicer/TRBP, Ago2 or Ago2/TRBP, immunodepletions were carried out and subsequently used in EMSAs (Figure 7). The efficiencies of the immunodepletions were also evaluated by western-blot analyses (Figure 7). HEK293 cell extracts immunodepleted of Dicer and/or TRBP (Id Dicer, Id TRBP, Id Dicer/TRBP), and Ago2 and TRBP (Id Ago2/TRBP) resulted in a loss of siRNA binding to the major

(a) hnRNP H siRNA sequences:

```
                5'-TTGTTGAACTTGAATCAGAAGATGAAGTCAAATTGGCCC-3'

hnRNP H #1 (H-1)   5'    AACUUGAAUCAGAAGAUGAAG
                   3'  ACUUGAACUUAGUCUUCUACU
hnRNP H #2 (H-2)   5'     ACUUGAAUCAGAAGAUGAAGU
                   3'   CUUGAACUUAGUCUUCUACUU
hnRNP H #3 (H-3)   5'      CUUGAAUCAGAAGAUGAAGUC
                   3'    UUGAACUUAGUCUUCUACUUC
hnRNP H #4 (H-4)   5'       UUGAAUCAGAAGAUGAAGUCA
                   3'     UGAACUUAGUCUUCUACUUCA
hnRNP H #5 (H-5)   5'        UGAAUCAGAAGAUGAAGUCAA
                   3'      GAACUUAGUCUUCUACUUCAG
hnRNP H #6 (H-6)   5'         GAAUCAGAAGAUGAAGUCAAA
                   3'       AACUUAGUCUUCUACUUCAGU
hnRNP H #7 (H-7)   5'          AAUCAGAAGAUGAAGUCAAAU
                   3'        ACUUAGUCUUCUACUUCAGUU
```

(b)

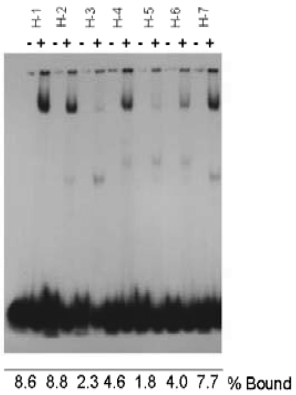

(c)

Targets:	psi-H1-S		psi-H1-AS	
	IC_{50} (pM)	95% confidence interval	IC_{50} (pM)	95% confidence interval
H1	9.03	6.98 to 11.7	5.40	4.90 to 5.96
H2	6.13	4.83 to 7.78	8.73	7.11 to 10.7
H3	29.7	20.5 to 43.0	7.66	5.22 to 11.2
H4	14.6	10.8 to 19.8	3.76	2.71 to 5.20
H5	71.6	51.7 to 99.0	9.75	8.91 to 10.8
H6	8.48	7.37 to 9.76	29.5	25.0 to 34.8
H7	5.75	5.17 to 6.39	10.0	9.02 to 11.1

Figure 4. Ribonucleoprotein complex formation and hnRNPH siRNA silencing. (**a**) A set of seven hnRNPH siRNAs targeting the hnRNP H site I (40). Upper strand is sense, lower strand is antisense. (**b**) Gel-shift assays. Anti-hnRNPH siRNAs were incubated with (+) or without (−) HCT116 cell extract and resolved in a 4.5% non-denaturing gel. The band shifts were quantified as described in Figure 1. The percent bound of each siRNA is shown under the corresponding gel lane. The assays were conducted multiple times with similar results, and a representative gel is shown here. (**c**) Determination of hnRNPH1 siRNA IC_{50} values. HCT116 cells were co-transfected with either psi-H1-Sense or -Antisense reporter plasmid and an siRNA ranging from 0.2 pM to 1.5 nM in serial dilutions (a minimal of 10 points measurements). Cell lysates collected 24-h post-transfection was subjected to the Dual-Luciferase Reporter Assay System (Promega) (Dose dependent target knockdown measurement curves are shown in Supplementary Figure S2).

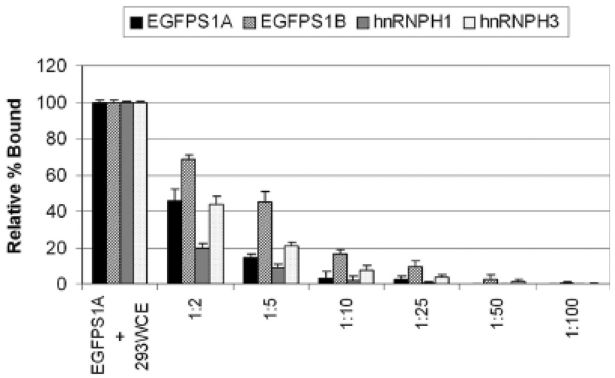

Figure 5. Competition assays. The specificity and requirement for siRNA duplexes for complex formation were examined using competition assays. Duplex requirements for complex formation were tested with radio-labeled EGFPS1A siRNA mixed with 2-, 5-, 10-, 25-, 50- or 100-fold molar excess of cold EGFPS1A, -B, hnRNPH1 or H3. Quantifications of the RNA–protein complexes were performed using densitometric scanning of the gel (Typhoon scanner).

complex. We were unable to immunodeplete Ago2 in the cell extract (Id Ago2, Figure 7), suggesting poor recognition of Ago2 by this antibody, perhaps due to interactions of Ago2 with other proteins in the extracts. Nevertheless, residual levels of Ago2 in Id Dicer, Id TRBP and Id Dicer/TRBP cell extracts had no effect on complex formation, consistent with the previous report that Ago2 does not associate with siRNA duplexes by itself (27). It is of interest to note that the combined use of anti-Ago2 and TRBP antibodies resulted in depletion of Ago2 in addition to Dicer and TRBP and this also abolished complex formation. This result is most likely a consequence of tight interactions among TRBP, Dicer and Ago2 (27). Most importantly we observed loss of siRNA gel shifts when the cell extracts were immunodepleted of Dicer, or the Dicer/TRBP heterodimer (Figure 7, lanes 4–6 and 8 in the left panel, and lanes 3–5 and 7 in the right panel). In total, these observations support Dicer as the siRNA-binding factor in the cell extracts.

To further explore the role of Dicer in the complex formation we replenished the Dicer immunodepleted extracts using purified recombinant Dicer and/or TRBP and tested for EGFPS1A complex formation (Figure 8). While rTRBP alone had no effect on complex restoration in both Id Dicer (lane 5) or Id TRBP cell extracts (lane 13), addition of rDicer or rDicer in combination with rTRBP (lanes 6, 7, 12 and 14) resulted in restoration of the siRNA/complex formation (Figures 8a–c).

Given the differential complex formation of several of the siRNAs described above, we next asked if Dicer alone can discriminate binding of a strong versus weak complex forming siRNA. To do this rDicer was incubated with either the EGFPS1-A or -B siRNA duplexes. As we observed in the high-molecular weight complex formation, rDicer alone showed differential binding affinities between these two siRNAs, forming a much stronger interaction with the EGFPS1A than with the EGFPS1B duplex (Supplementary Figure S3). Although rDicer aggregated and was poorly resolved in the composite gel, the differential binding was reproducible.

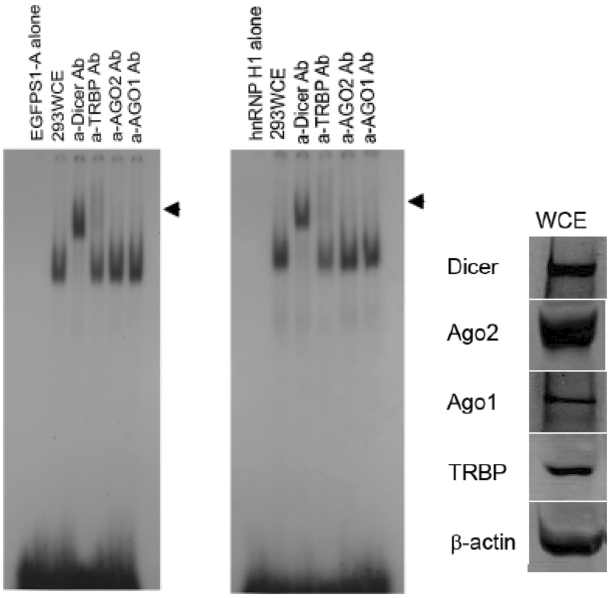

Figure 6. Analysis of proteins comprising the complex. Super shift assays. α-Dicer, α-TRBP, α-Ago2 or α-Ago1 antibodies were added to the HEK293 cell extract and incubated for 15 min prior to addition of either EGFPS1A or hnRNPH1 siRNA. Western analyses of proteins detected with the antibodies were also shown on the right. Of total protein, 50 μg for detection of Dicer and Ago1 or 150 μg for Ago2, TRBP and β-actin was loaded on 8% SDS–PAGE gels.

To dissect the relative roles of Dicer, Ago2 and TRBP in selective incorporation of siRNAs *in vivo*, we used RNAi to knockdown each of these proteins and assayed for EGFPS1A-mediated target knockdown using the panel of EGFPS1A siRNAs that differ in their 3′-end structures (depicted and tested in Figure 1). If Dicer binding initially determines the 3′-end structure and guide strand selection, the differential efficiencies of the EGFPS1A variants should be absent in Dicer knockdown cells. Of course knockdown of Ago2 would also reduce RNAi overall since it is required for the RNAi effector step of cleaving the target transcripts. We compared the knockdowns of EGFP via the EGFPS1A panel in HEK293 in cells pre-treated with siRNAs targeting Dicer, Ago2 or TRBP (Figure 9). Consistent with a key role for Dicer in siRNA selection, the previously observed differences in knockdown efficiencies of the EGFPS1A variants were substantially reduced in cells pre-treated with the anti-Dicer siRNA. In these cells, we determined that levels of Dicer and Ago2 expression were repressed ~85% and 65%, respectively (Supplementary Figure S4). Although TRBP mRNA levels were reduced by ~60%, the effects of this reduction on the differential knockdown efficiencies by the EGFPS1A panel were minimal, which is

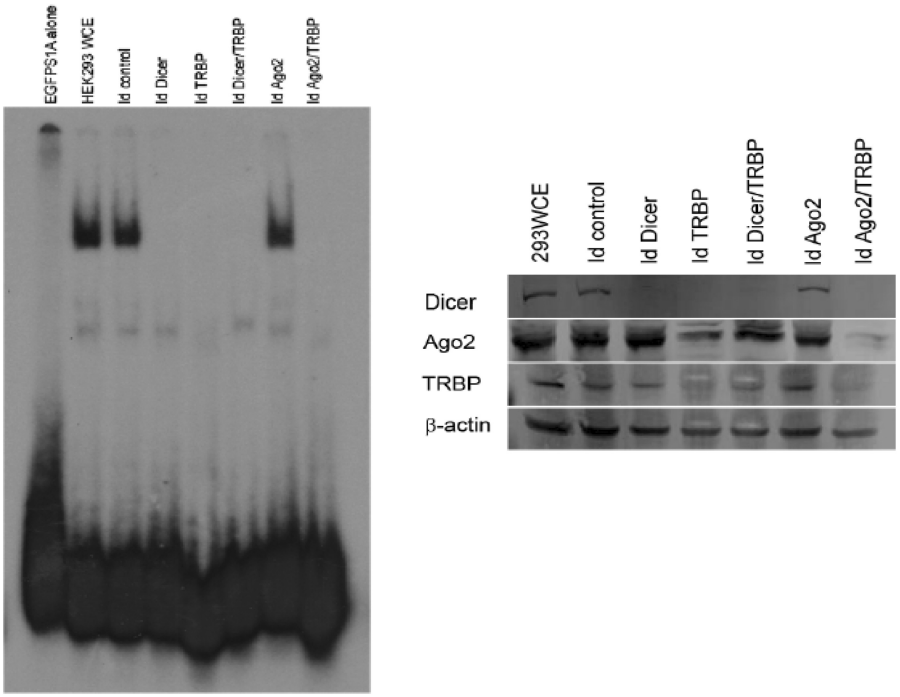

Figure 7. Analysis of RISC components required in high-molecular-complex formation. Gel-shift assays. EGFPS1A duplex was incubated with HEK293 cell extracts immunodepleted of Dicer (Id Dicer), TRBP (Id TRBP), Dicer and TRBP (Id Dicer/TRBP), Ago2 (Id Ago2) or Ago2 and TRBP (Id Ago2/TRBP). Evaluation of immunodepletion of RISC proteins with western blot analyses was shown on the right. Of Id cell extracts, 150 μg were loaded on a 8% SDS–PAGE gel. Pre-immune serum was used as an immunodepletion control.

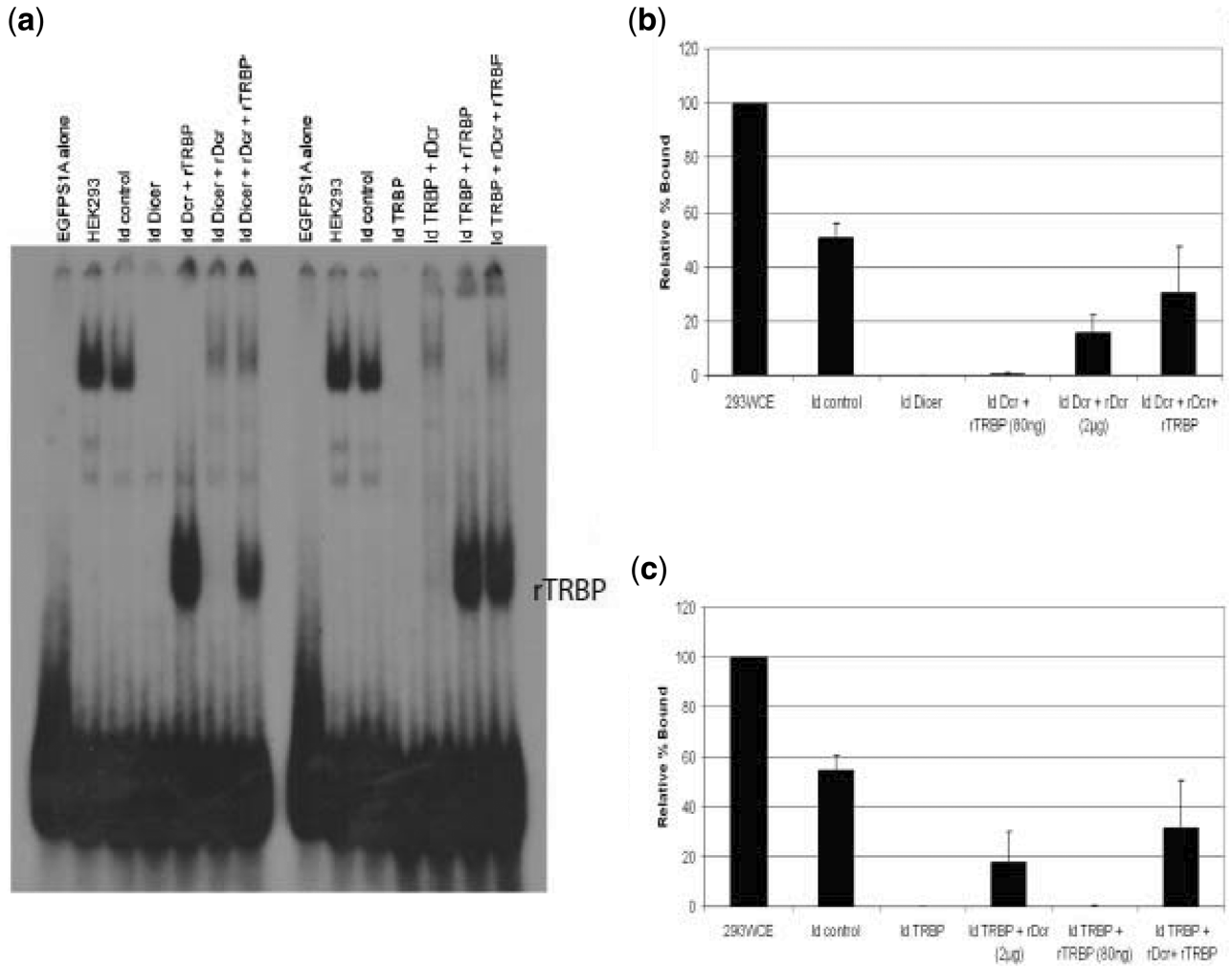

Figure 8. Analysis of siRNA–RISC complex formation. (**a**) Reconstitution of the siRNA complex with recombinant proteins. Id Dicer (left) or Id TRBP (right) cell extracts were mixed with 2 µg of recombinant Dicer, 80 ng of recombinant TRBP or both proteins to rescue complex formation. (**b** and **c**) Percent-bound-reconstituted siRNA complexes were calculated relative to the HEK293 WCE which was set as 100%.

consistent with our EMSA results (Figures 7 and 8). To further validate these results, we also tested the effect of Dicer knockdown on siRNA-triggered gene silencing by comparing knockdown efficiencies of hnRNPH5 and H6 in siDicer-treated HEK293 cells (Supplementary Figure S5). When the siRNAs were co-transfected with the psi-H1-S or psi-H1-AS reporter plasmid at 200 pM, asymmetric knockdowns of the sense or antisense targets by the siRNA duplexes were observed; however knockdown efficiencies of hnRNPH5 and H6 siRNAs were substantially reduced in siDicer treated cells (Supplementary Figure S5). Our observations indicate that the overall efficacies of the siRNAs were diminished in the Dicer knockdown cells, consistent with previous observations (27,56), which is most likely a consequence of disruption of the RLC.

To discriminate the selective binding aspect of Dicer from direct incorporation of the siRNAs into Ago2, we modified EGFPS1A to generate an asymmetric 27/25-nt-long Dicer substrate form (DsiRNA)—a blunt end with two deoxyribonucleotide bases at the 3′-end of the passenger strand—forcing the duplex to be bound and undergo Dicer cleavage activity. EGFPS1B was also modified to a DsiRNA form for direct comparison, and the IC_{50} values were determined for both DsiRNAs (Figure 10a and b). For both EGFPS1A and B DsiRNAs, the strand harboring the 2-nt 3′ overhang was predominantly selected as the guide strand ($IC_{50,\ Dsi\text{-}S1A\text{-}AS}$ = 31.9 pM, $IC_{50,\ Dsi\text{-}S1A\text{-}Sense}$ = 101 pM; $IC_{50,\ Dsi\text{-}S1B\text{-}AS}$ = 27.5 pM, $IC_{50,\ Dsi\text{-}S1B\text{-}Sense}$ = 433 pM), consistent with previous observations (40). In contrast, the dominant selection of the antisense strand (relative to the sense EGFP target) was absent or less pronounced with the use of 19 + 2 siRNAs. Both the dsiRNAs and siRNAs form dicer-dependent complexes in whole-cell extracts (57) (Supplementary Figure S6). These results support a model in which the orientation of Dicer binding to its substrates sets the preference for which strand will be chosen to act as the guide strand. Taken together, our observations suggest that the initial Dicer–DsiRNA interaction is an important determinant for establishing siRNA-strand selection in RISC and ultimately

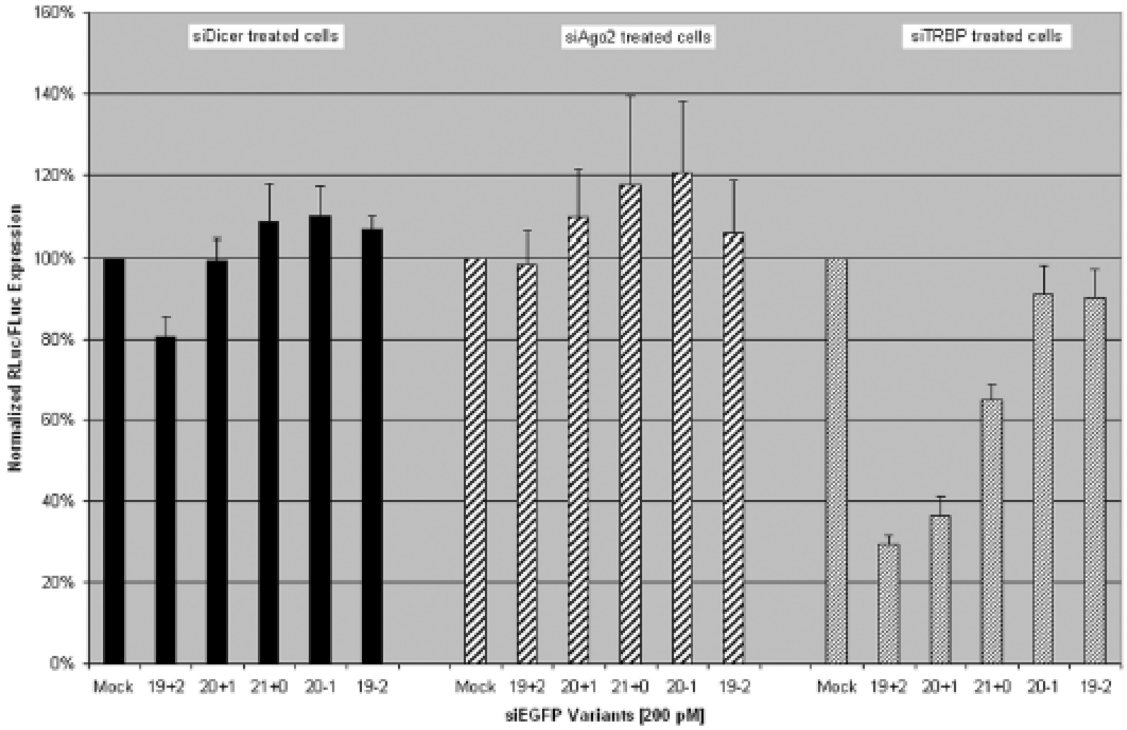

Figure 9. The effect of 3′ overhang on RISC function in Dicer kd, Ago2 kd and TRBP kd cells. Efficiencies of target downregulation by four variants of EGFPS1A siRNA (Figure 1) were evaluated using Dual Luciferase assays with siDicer, siAgo2 or siTRBP treated HEK293 cells. To determine effects of Dicer, Ago2 or TRBP knockdowns on the silencing activity of the siEGFPS1A variants described in Figure 1, HEK293 cells were treated with 40 nM siDicer, siAgo2 or siTRBP for 2 days prior to the co-transfection. For the second round of transfection, Dicer kd, Ago2 kd or TRBP kd cells were transfected with the psi-EGFP-S1 sense reporter and 200 pM siEGFPS1A variants. Target-specific *Renilla* luciferase expression was normalized to the control Firefly luciferase expression for all replicates (determined from four co-transfections).

the potency of the siRNAs. The Dicer substrates force Dicer to enter the RNA via its PAZ domain and the 2-base 3′ overhang of the Dicer substrate whereas 19 + 2 siRNAs allow Dicer to bind from either end using the 2-base 3′ overhang for PAZ domain interactions.

DISCUSSION

We have used siRNA binding to a high-molecular-weight complex in whole-cell extracts to better understand what cellular factors are involved in the initial binding and discriminatory selection of highly functional versus poorly functional siRNAs. In particular, we have been interested in what happens to siRNAs following transfection into cultured cells. We find that the extent of siRNA complex formation reflects siRNA-directed overall target knockdown efficiency in cultured cells. Using antibodies to core RNAi proteins to determine the key proteins of the complex, we find that it minimally consists of Dicer/TRBP, presumably as the pre-RLC. Our observations suggest that human RISC silencing efficiency with exogenously supplied siRNAs reflects the extent of siRNA-pre-RLC formation.

Previously, mammalian Dicer was shown to be dispensable for RISC assembly and siRNA-mediated cleavage of target RNA transcripts (41–43). In contrast, the absence of a functional mouse Dicer resulted in a lack of shRNA-mediated RNAi (43), showing that Dicer-cleavage activity was necessary to generate the siRNAs from this precursor. The lack of a Dicer requirement for pre-formed siRNA function led to the conclusion that only Ago2 was required for siRNA selection. Conversely, two groups demonstrated that the absence of Dicer abolished gene silencing effects (27,56). Our results suggest that when present, Dicer itself binds siRNAs that mimic the products of Dicer cleavage (19 bp + 2-nt 3′ overhangs) and Dicer can serve as a 'gate-keeper' discriminating between potent and non-potent siRNAs by selective binding of the siRNAs in the pre-RLC.

Schwarz et al. reported that 2–4 bp on both ends of a siRNA are important for their relative loading efficiency into RISC in *Drosophila* (35). Our calculated duplex end free energies for siRNAs used in this study (Table 1) are consistent with these observations. Moreover, we observed that in general, siRNAs with thermodynamically unstable base pairs at both ends effectively form high-molecular-weight complexes in cell extracts and have better overall silencing efficiencies. These observations suggest that the thermodynamic properties of 2–4 bp on both ends of effective siRNAs are used as functional determinants by the pre-RLC and determine overall silencing efficiency in humans as well.

It is widely known that siRNAs targeting the same region of a target mRNA can have a wide range of

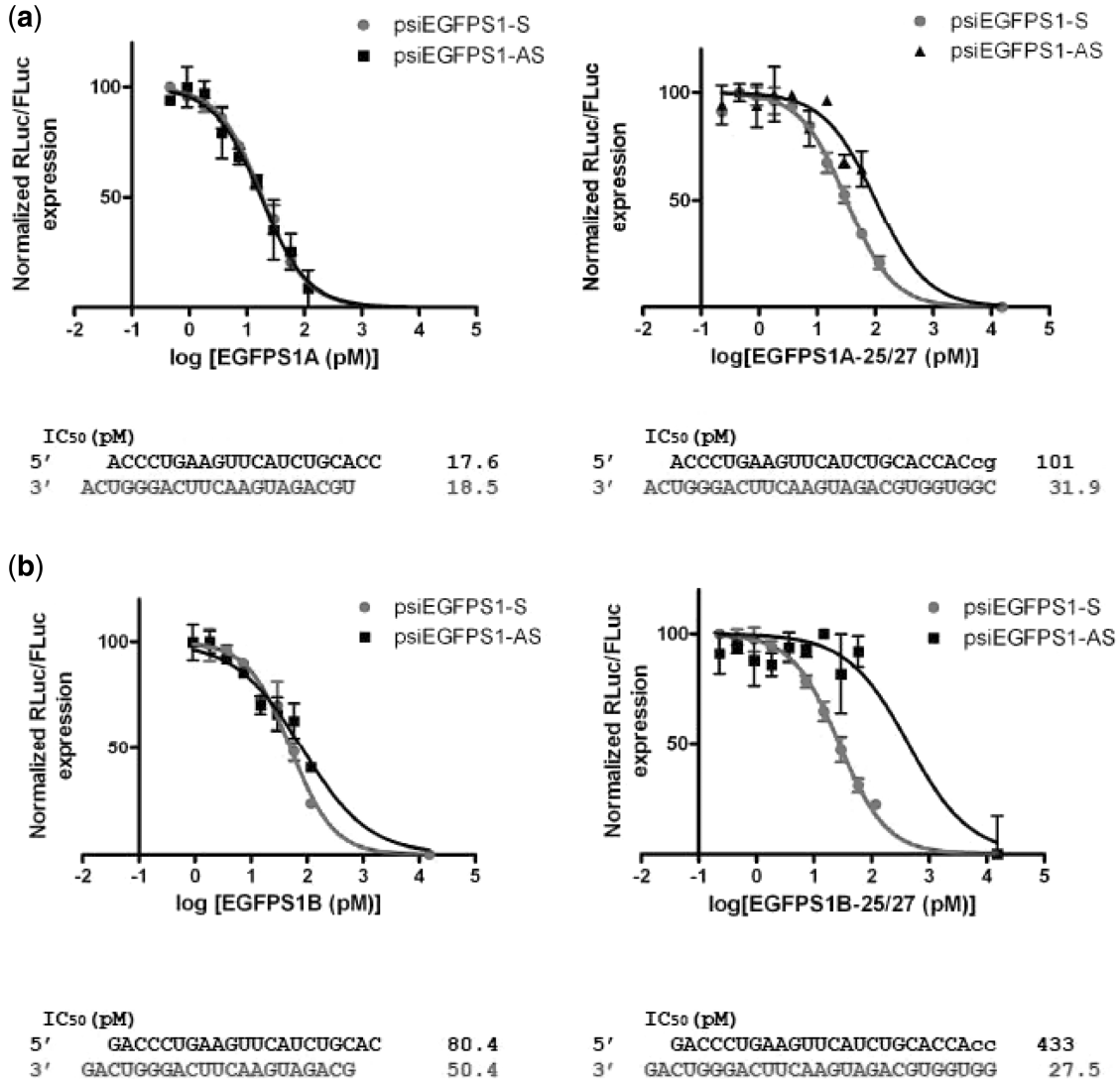

Figure 10. Comparative analyses of guide strand selection for 21-mer and 25/27-mer Dicer substrate siRNAs. Target knockdowns for sense and antisense strands of siRNA EGFPS1A (**a**) and EGFPS1B (**b**) in 21-mer and Dicer substrate formats were carried out using co-transfections of the siRNAs with either the psi-EGFP-S sense reporter (red) or psi-EGFP-AS antisense reporter (black) in HEK293 cells. For both targets the 21-nt EGFPS1 siRNAs (left) or 25/27 DsiRNAs (right) were tested at various concentrations. Target-specific *Renilla* luciferase expression was normalized to the control Firefly luciferase expression for all replicates (determined from multiple co-transfections). Sequences and IC_{50} values of each siRNA are shown. For the Dicer substrate siRNAs, the lower case letters represent deoxyribonucleotide containing bases which block Dicer entry.

potencies. To circumvent this obstacle, reported siRNA features such as an A at position 3 or 19 and 30–50% overall GC content in the passenger strand (37,39,52–54) are widely used to predict potent siRNAs in addition to thermodynamic end properties. However, the importance of the AU base pair at these positions remained elusive. Using two sets of siRNAs targeting EGFP site I and hnRNP H site I (40), we observed that siRNAs containing an A:U base pair at positions 1 and/or 19 result in more effective binding to the high-molecular-weight complex than those with C:G pairs at these positions. This finding is consistent with the previous report of Katoh and Suzuki (58) which suggested that an AU base pair at these positions makes the siRNA a good substrate for the pre-RLC interaction and selection as an effective siRNA for target downregulation.

The manipulations of the 2-nt 3′ overhangs, which resulted in reductions in target downregulation (Figure 1) verify that the presence of a 1- or 2-nt 3′ overhang is required not only for efficient binding to the high-molecular-weight complex, but is also required for efficient target downregulation. Previously, Pellino *et al.* (55) reported that the complex observed with HEK293 cell extracts contained Dicer. Our siRNA gel shift and binding assays along with the immunodepletion assays in HCT116 and HEK293 cell extracts demonstrate that Dicer is required for siRNA binding in these extracts, a result which is consistent with reports that the initial siRNA–Dicer interaction is via the 2-nt 3′ overhang (59,60).

The marked differences in Dicer/TRBP binding to siRNAs and the correlations with efficacy of target

knockdown in cell culture, even for siRNAs differing by only a single nucleotide in sequence, point to the importance of understanding how siRNAs are selected for entry into RISC. Understanding the rules for effective siRNA design is further complicated by the fact that siRNAs which do not bind to Dicer can also be incorporated into RISC (41–43). We propose though that when Dicer is present it will preferentially bind and select siRNAs harboring structurally favorable features, and this interaction leads to the subsequent handoff step to Ago2.

Selective binding of Dicer to siRNAs could potentially determine the strand to be incorporated as a guide strand. The binding of the PAZ domain to a Dicer substrate allows the catalytic domain to interact with the opposite end of the dsRNA. Studies of the interaction of the human Dicer catalytic site with the PIWI domain of Ago2 (61) and the binding of the *Archaeoglobus fulgidus* PIWI protein with the 5′-end of the guide strand in the crystal structure (62) suggest the coupling of the initiation and effector steps of RNAi. The handoff of the guide strand from Dicer to Ago2 via the Dicer-catalytic domain could explain not only why Dicer processing of longer precursors often increases the efficacy of processed siRNAs (40,63), but also why the 5′-end of the siRNA within RISC leads to and determines the stable association of RISC and the target RNA (64). In this regard, Dicer substrates in the studies of Rose *et al.* (40) have a blunt end with two deoxybases at the 3′-end of the passenger strand, which precludes Dicer PAZ domain interactions from that end of the duplex. The polarity of Dicer entry from the end harboring the 2-base 3′ overhang results in substantially reduced function of the passenger strand relative to that observed with the corresponding 19 + 2 siRNA (Figure 10). Moreover, a single-nucleotide shift in the siRNA relative to the target site also resulted in a strong bias in guide strand selection for the dsiRNAs as demonstrated by EGFPS1A-25/27 ($IC_{50,\ Dsi\text{-}S1A\text{-}Sense}$ = 101 pM) and EGFPS1B-25/27 DsiRNAs ($IC_{50,\ Dsi\text{-}S1B\text{-}Sese}$ = 433 pM) (Figure 10). Thus, Dicer interaction with the 2-nt 3′ overhang is an important step in Dicer binding, and for 19 + 2 siRNAs Dicer can bind in two orientations. Nevertheless, the thermodynamic end properties of the siRNAs also influence Dicer binding as we have demonstrated.

Recent single-particle EM analyses of the RLC-containing Dicer/TRBP/Ago2, show that Ago2 is associated with the C-terminal domain of Dicer, while TRBP is associated with the N-terminal or helicase domain of Dicer (65,66). This structural configuration would facilitate Dicer handoff of the 5′-end of the guide strand to Ago2. Our observations that Dicer binds selectively to 2-base 3′ overhangs, most likely via the PAZ domain, would orient the enzyme such that the C-terminal portion of the enzyme is associated with the 5′-end of the guide strand to facilitate handoff of the guide strand to Ago2. An important observation is that the stability of Dicer binding to an siRNA is not solely mediated by the 3′ 2-base overhang, but obviously involves interactions with the duplex itself. This is made evident by the fact that many of the siRNAs used in our binding analyses contain the 2-base overhang but are not bound strongly to the Dicer-containing complex.

Thus far, the binding efficiency of Dicer/TRBP to pre-miRNAs appears to be maintained regardless of whether or not the pre-miRNA can be cleaved by Dicer (67). Our work and that of Pellino et al. (55) demonstrate that Dicer/TRBP can bind to siRNAs as well. However, these observations are in contrast to a previous study that human Dicer is incapable of siRNA binding (68). One possible explanation for this discrepancy is that the siRNA used in the previous study may fall into the group of siRNAs that are weak binders to the pre-RLC—similar to the poor binding siRNAs tested in our study.

While immunodepletion of Dicer (Id Dicer) left-residual TRBP, Id of TRBP resulted in nearly complete depletion of Dicer in the HEK 293 cell extracts, as did co-Id of Dicer/TRBP. These results indicate that the majority of Dicer is bound to TRBP and that distinctive roles of Dicer and TRBP augment each other to function as the pre-RLC. Id of Ago2/TRBP resulted in immunodepletion of Dicer, TRBP and Ago2 (Figure 7), suggesting that TRBP functions as a bridge between Dicer and Ago2.

We have demonstrated that for many siRNAs what we deemed as the passenger strand could be more effective at target knockdown than the desired antisense guide strand. Since Dicer/TRBP binding to a siRNA duplex determines the strand to be selected as the guide strand, off-targeting will often be a consequence of both strands being incorporated into RISC. Thus the two strands of a siRNA can also compete with one another for incorporation into RISC following Dicer selection, thereby potentially reducing the potencies of both.

In conclusion our results demonstrate that human Dicer plays an important role in selection of efficacious siRNAs via direct binding to siRNAs that harbor certain structural features, which include the 2-nt 3′ overhangs and the thermodynamically unstable base pairing at the ends of the duplex. These results are similar yet distinct from *Drosophila* in which R2D2 and Dcr-2 bind to the thermodynamically stable and unstable ends of siRNA duplexes, respectively. Our results demonstrate that the human Dicer enzyme can recognize and selectively bind siRNAs with thermodynamically favorable termini. Our results demonstrate that an often overlooked feature of 19 + 2 siRNAs is the ability of both strands to be chosen for RISC entry. This is sometimes observed for miRNAs as well, but often only one strand serves as the guide. In this regard, Dicer substrate siRNAs mimic the miRNA pathway, providing strong polarity for guide strand selection, perhaps a useful attribute for minimizing off target effects and competition between the two strands for entry into RISC.

SUPPLEMENTARY DATA

Supplementary Data are available at NAR Online.

ACKNOWLEDGEMENTS

The authors acknowledge members of the Rossi laboratory for helpful discussions and support, especially Lisa

Scherer for the critical reading of this article. They are grateful for the suggestions of Y. Chen, R.J. Lin, J Shively and J. Termini.

FUNDING

Norwegian Research Council (a postdoctoral fellowship to M.A.); Arnold and Mabel Beckman Foundation (to D.K.); National Institutes of Health (grants AI29329, AI42552 and HL074704 to J.J.R.). Funding for open access charges: National Institutes of Health National Heart Lung and Blood Institute and National Institute of Allergy and Infectious Diseases.

Conflict of interest statement. M.A.B. is employed by IDT DNA, which manufactures siRNAs and dicer substrate siRNAs. J.J.R. is chairman of the SAB at Dicerna Pharmacueticals which uses Dicer substrate siRNAs.

REFERENCES

1. Hammond,S.M., Bernstein,E., Beach,D. and Hannon,G.J. (2000) An RNA-directed nuclease mediates post-transcriptional gene silencing in Drosophila cells. *Nature*, **404**, 293–296.
2. Hannon,G.J. (2002) RNA interference. *Nature*, **418**, 244–251.
3. Bernstein,E., Caudy,A.A., Hammond,S.M. and Hannon,G.J. (2001) Role for a bidentate ribonuclease in the initiation step of RNA interference. *Nature*, **409**, 363–366.
4. Liu,J., Carmell,M.A., Rivas,F.V., Marsden,C.G., Thomson,J.M., Song,J.J., Hammond,S.M., Joshua-Tor,L. and Hannon,G.J. (2004) Argonaute2 is the catalytic engine of mammalian RNAi. *Science*, **305**, 1437–1441.
5. Meister,G., Landthaler,M., Patkaniowska,A., Dorsett,Y., Teng,G. and Tuschl,T. (2004) Human Argonaute2 mediates RNA cleavage targeted by miRNAs and siRNAs. *Mol. Cell*, **15**, 185–197.
6. Rivas,F.V., Tolia,N.H., Song,J.J., Aragon,J.P., Liu,J., Hannon,G.J. and Joshua-Tor,L. (2005) Purified Argonaute2 and an siRNA form recombinant human RISC. *Nat. Struct. Mol. Biol.*, **12**, 340–349.
7. Elbashir,S.M., Harborth,J., Lendeckel,W., Yalcin,A., Weber,K. and Tuschl,T. (2001) Duplexes of 21-nucleotide RNAs mediate RNA interference in cultured mammalian cells. *Nature*, **411**, 494–498.
8. Elbashir,S.M., Lendeckel,W. and Tuschl,T. (2001) RNA interference is mediated by 21- and 22-nucleotide RNAs. *Genes Dev.*, **15**, 188–200.
9. Elbashir,S.M., Martinez,J., Patkaniowska,A., Lendeckel,W. and Tuschl,T. (2001) Functional anatomy of siRNAs for mediating efficient RNAi in Drosophila melanogaster embryo lysate. *Embo J.*, **20**, 6877–6888.
10. Zamore,P.D., Tuschl,T., Sharp,P.A. and Bartel,D.P. (2000) RNAi: double-stranded RNA directs the ATP-dependent cleavage of mRNA at 21 to 23 nucleotide intervals. *Cell*, **101**, 25–33.
11. Bagga,S., Bracht,J., Hunter,S., Massirer,K., Holtz,J., Eachus,R. and Pasquinelli,A.E. (2005) Regulation by let-7 and lin-4 miRNAs results in target mRNA degradation. *Cell*, **122**, 553–563.
12. Grimson,A., Farh,K.K., Johnston,W.K., Garrett-Engele,P., Lim,L.P. and Bartel,D.P. (2007) MicroRNA targeting specificity in mammals: determinants beyond seed pairing. *Mol. cell*, **27**, 91–105.
13. Brennecke,J., Stark,A., Russell,R.B. and Cohen,S.M. (2005) Principles of microRNA-target recognition. *PLoS Biol.*, **3**, e85.
14. Lee,R.C., Feinbaum,R.L. and Ambros,V. (1993) The C. elegans heterochronic gene lin-4 encodes small RNAs with antisense complementarity to lin-14. *Cell*, **75**, 843–854.
15. Lewis,B.P., Burge,C.B. and Bartel,D.P. (2005) Conserved seed pairing, often flanked by adenosines, indicates that thousands of human genes are microRNA targets. *Cell*, **120**, 15–20.
16. Behm-Ansmant,I., Rehwinkel,J., Doerks,T., Stark,A., Bork,P. and Izaurralde,E. (2006) mRNA degradation by miRNAs and GW182 requires both CCR4:NOT deadenylase and DCP1:DCP2 decapping complexes. *Genes Dev.*, **20**, 1885–1898.
17. Giraldez,A.J., Mishima,Y., Rihel,J., Grocock,R.J., Van Dongen,S., Inoue,K., Enright,A.J. and Schier,A.F. (2006) Zebrafish MiR-430 promotes deadenylation and clearance of maternal mRNAs. *Science*, **312**, 75–79.
18. Wu,L., Fan,J. and Belasco,J.G. (2006) MicroRNAs direct rapid deadenylation of mRNA. *Proc. Natl Acad. Sci. USA*, **103**, 4034–4039.
19. Liu,Q., Rand,T.A., Kalidas,S., Du,F., Kim,H.E., Smith,D.P. and Wang,X. (2003) R2D2, a bridge between the initiation and effector steps of the Drosophila RNAi pathway. *Science*, **301**, 1921–1925.
20. Lee,Y.S., Nakahara,K., Pham,J.W., Kim,K., He,Z., Sontheimer,E.J. and Carthew,R.W. (2004) Distinct roles for Drosophila Dicer-1 and Dicer-2 in the siRNA/miRNA silencing pathways. *Cell*, **117**, 69–81.
21. Forstemann,K., Tomari,Y., Du,T., Vagin,V.V., Denli,A.M., Bratu,D.P., Klattenhoff,C., Theurkauf,W.E. and Zamore,P.D. (2005) Normal microRNA maturation and germ-line stem cell maintenance requires Loquacious, a double-stranded RNA-binding domain protein. *PLoS Biol.*, **3**, e236.
22. Saito,K., Ishizuka,A., Siomi,H. and Siomi,M.C. (2005) Processing of pre-microRNAs by the Dicer-1-Loquacious complex in Drosophila cells. *PLoS Biol.*, **3**, e235.
23. Liu,X., Jiang,F., Kalidas,S., Smith,D. and Liu,Q. (2006) Dicer-2 and R2D2 coordinately bind siRNA to promote assembly of the siRISC complexes. *RNA*, **12**, 1514–1520.
24. Bernstein,E., Kim,S.Y., Carmell,M.A., Murchison,E.P., Alcorn,H., Li,M.Z., Mills,A.A., Elledge,S.J., Anderson,K.V. and Hannon,G.J. (2003) Dicer is essential for mouse development. *Nat. Genet.*, **35**, 215–217.
25. Hutvagner,G., McLachlan,J., Pasquinelli,A.E., Balint,E., Tuschl,T. and Zamore,P.D. (2001) A cellular function for the RNA-interference enzyme Dicer in the maturation of the let-7 small temporal RNA. *Science*, **293**, 834–838.
26. MacRae,I.J., Ma,E., Zhou,M., Robinson,C.V. and Doudna,J.A. (2008) In vitro reconstitution of the human RISC-loading complex. *Proc. Natl Acad. Sci. USA*, **105**, 512–517.
27. Chendrimada,T.P., Gregory,R.I., Kumaraswamy,E., Norman,J., Cooch,N., Nishikura,K. and Shiekhattar,R. (2005) TRBP recruits the Dicer complex to Ago2 for microRNA processing and gene silencing. *Nature*, **436**, 740–744.
28. Gregory,R.I., Chendrimada,T.P., Cooch,N. and Shiekhattar,R. (2005) Human RISC couples microRNA biogenesis and posttranscriptional gene silencing. *Cell*, **123**, 631–640.
29. Haase,A.D., Jaskiewicz,L., Zhang,H., Laine,S., Sack,R., Gatignol,A. and Filipowicz,W. (2005) TRBP, a regulator of cellular PKR and HIV-1 virus expression, interacts with Dicer and functions in RNA silencing. *EMBO Reports*, **6**, 961–967.
30. Lee,Y., Hur,I., Park,S.Y., Kim,Y.K., Suh,M.R. and Kim,V.N. (2006) The role of PACT in the RNA silencing pathway. *EMBO J.*, **25**, 522–532.
31. Meister,G., Landthaler,M., Peters,L., Chen,P.Y., Urlaub,H., Luhrmann,R. and Tuschl,T. (2005) Identification of novel argonaute-associated proteins. *Curr. Biol.*, **15**, 2149–2155.
32. Chendrimada,T.P., Finn,K.J., Ji,X., Baillat,D., Gregory,R.I., Liebhaber,S.A., Pasquinelli,A.E. and Shiekhattar,R. (2007) MicroRNA silencing through RISC recruitment of eIF6. *Nature*, **447**, 823–828.
33. Robb,G.B. and Rana,T.M. (2007) RNA helicase A interacts with RISC in human cells and functions in RISC loading. *Mol. Cell*, **26**, 523–537.
34. Khvorova,A., Reynolds,A. and Jayasena,S.D. (2003) Functional siRNAs and miRNAs exhibit strand bias. *Cell*, **115**, 209–216.
35. Schwarz,D.S., Hutvagner,G., Du,T., Xu,Z., Aronin,N. and Zamore,P.D. (2003) Asymmetry in the assembly of the RNAi enzyme complex. *Cell*, **115**, 199–208.
36. Tomari,Y., Matranga,C., Haley,B., Martinez,N. and Zamore,P.D. (2004) A protein sensor for siRNA asymmetry. *Science*, **306**, 1377–1380.

37. Reynolds,A., Leake,D., Boese,Q., Scaringe,S., Marshall,W.S. and Khvorova,A. (2004) Rational siRNA design for RNA interference. *Nat. Biotechnol.*, **22**, 326–330.
38. Amarzguioui,M., Holen,T., Babaie,E. and Prydz,H. (2003) Tolerance for mutations and chemical modifications in a siRNA. *Nucleic Acids Res.*, **31**, 589–595.
39. Ui-Tei,K., Naito,Y., Takahashi,F., Haraguchi,T., Ohki-Hamazaki,H., Juni,A., Ueda,R. and Saigo,K. (2004) Guidelines for the selection of highly effective siRNA sequences for mammalian and chick RNA interference. *Nucleic Acids Res.*, **32**, 936–948.
40. Rose,S.D., Kim,D.H., Amarzguioui,M., Heidel,J.D., Collingwood,M.A., Davis,M.E., Rossi,J.J. and Behlke,M.A. (2005) Functional polarity is introduced by Dicer processing of short substrate RNAs. *Nucleic Acids Res.*, **33**, 4140–4156.
41. Murchison,E.P., Partridge,J.F., Tam,O.H., Cheloufi,S. and Hannon,G.J. (2005) Characterization of Dicer-deficient murine embryonic stem cells. *Proc. Natl Acad. Sci. USA*, **102**, 12135–12140.
42. Martinez,J., Patkaniowska,A., Urlaub,H., Luhrmann,R. and Tuschl,T. (2002) Single-stranded antisense siRNAs guide target RNA cleavage in RNAi. *Cell*, **110**, 563–574.
43. Kanellopoulou,C., Muljo,S.A., Kung,A.L., Ganesan,S., Drapkin,R., Jenuwein,T., Livingston,D.M. and Rajewsky,K. (2005) Dicer-deficient mouse embryonic stem cells are defective in differentiation and centromeric silencing. *Genes Dev.*, **19**, 489–501.
44. Tomari,Y., Du,T. and Zamore,P.D. (2007) Sorting of Drosophila small silencing RNAs. *Cell*, **130**, 299–308.
45. Birmingham,A., Anderson,E.M., Reynolds,A., Ilsley-Tyree,D., Leake,D., Fedorov,Y., Baskerville,S., Maksimova,E., Robinson,K., Karpilow,J. *et al.* (2006) 3′ UTR seed matches, but not overall identity, are associated with RNAi off-targets. *Nat. Methods*, **3**, 199–204.
46. Fedorov,Y., Anderson,E.M., Birmingham,A., Reynolds,A., Karpilow,J., Robinson,K., Leake,D., Marshall,W.S. and Khvorova,A. (2006) Off-target effects by siRNA can induce toxic phenotype. *RNA (New York, NY)*, **12**, 1188–1196.
47. Lin,X., Ruan,X., Anderson,M.G., McDowell,J.A., Kroeger,P.E., Fesik,S.W. and Shen,Y. (2005) siRNA-mediated off-target gene silencing triggered by a 7 nt complementation. *Nucleic Acids Res.*, **33**, 4527–4535.
48. Clark,P.R., Pober,J.S. and Kluger,M.S. (2008) Knockdown of TNFR1 by the sense strand of an ICAM-1 siRNA: dissection of an off-target effect. *Nucleic Acids Res.*, **36**, 1081–1097.
49. Castanotto,D., Sakurai,K., Lingeman,R., Li,H., Shively,L., Aagaard,L., Soifer,H., Gatignol,A., Riggs,A. and Rossi,J.J. (2007) Combinatorial delivery of small interfering RNAs reduces RNAi efficacy by selective incorporation into RISC. *Nucleic Acids Res.*, **35**, 5154–5164.
50. Daher,A., Laraki,G., Singh,M., Melendez-Peña,C.E., Bannwarth,S., Peters,A.H., Meurs,E.F., Braun,R.E., Patel,R.C. and Gatignol,A. (2009) TRBP control of PACT-induced phosphorylation of protein kinase R is reversed by stress. *Mol. Cell. Biol.*, **29**, 254–265.
51. Daviet,L., Erard,M., Dorin,D., Duarte,M., Vaquero,C. and Gatignol,A. (2000) Analysis of a binding difference between the two dsRNA-binding domains in TRBP reveals the modular function of a KR-helix motif. *Eur. J. Biochem./FEBS*, **267**, 2419–2431.
52. Amarzguioui,M. and Prydz,H. (2004) An algorithm for selection of functional siRNA sequences. *Biochem. Biophys. Res. Commun.*, **316**, 1050–1058.
53. Holen,T. (2006) Efficient prediction of siRNAs with siRNArules 1.0: an open-source JAVA approach to siRNA algorithms. *RNA*, **12**, 1620–1625.
54. Saetrom,P. and Snove,O. Jr (2004) A comparison of siRNA efficacy predictors. *Biochem. Biophys. Res. Commun.*, **321**, 247–253.
55. Pellino,J.L., Jaskiewicz,L., Filipowicz,W. and Sontheimer,E.J. (2005) ATP modulates siRNA interactions with an endogenous human Dicer complex. *RNA*, **11**, 1719–1724.
56. Doi,N., Zenno,S., Ueda,R., Ohki-Hamazaki,H., Ui-Tei,K. and Saigo,K. (2003) Short-interfering-RNA-mediated gene silencing in mammalian cells requires Dicer and eIF2C translation initiation factors. *Curr. Biol.*, **13**, 41–46.
57. Soifer,H.S., Sano,M., Sakurai,K., Chomchan,P., Saetrom,P., Sherman,M.A., Collingwood,M.A., Behlke,M.A. and Rossi,J.J. (2008) A role for the Dicer helicase domain in the processing of thermodynamically unstable hairpin RNAs. *Nucleic Acids Res.*, **36**, 6511–6522.
58. Katoh,T. and Suzuki,T. (2007) Specific residues at every third position of siRNA shape its efficient RNAi activity. *Nucleic Acids Res.*, **35**, e27.
59. Song,J.J., Liu,J., Tolia,N.H., Schneiderman,J., Smith,S.K., Martienssen,R.A., Hannon,G.J. and Joshua-Tor,L. (2003) The crystal structure of the Argonaute2 PAZ domain reveals an RNA binding motif in RNAi effector complexes. *Nat. Struct. Biol.*, **10**, 1026–1032.
60. MacRae,I.J., Zhou,K. and Doudna,J.A. (2007) Structural determinants of RNA recognition and cleavage by Dicer. *Nat. Struct. Mol. Biol.*, **14**, 934–940.
61. Tahbaz,N., Kolb,F.A., Zhang,H., Jaronczyk,K., Filipowicz,W. and Hobman,T.C. (2004) Characterization of the interactions between mammalian PAZ PIWI domain proteins and Dicer. *EMBO Reports*, **5**, 189–194.
62. Kolb,F.A., Zhang,H., Jaronczyk,K., Tahbaz,N., Hobman,T.C. and Filipowicz,W. (2005) Human dicer: purification, properties, and interaction with PAZ PIWI domain proteins. *Methods Enzymol.*, **392**, 316–336.
63. Kim,D.H., Behlke,M.A., Rose,S.D., Chang,M.S., Choi,S. and Rossi,J.J. (2005) Synthetic dsRNA Dicer substrates enhance RNAi potency and efficacy. *Nat. Biotechnol.*, **23**, 222–226.
64. Ameres,S.L., Martinez,J. and Schroeder,R. (2007) Molecular basis for target RNA recognition and cleavage by human RISC. *Cell*, **130**, 101–112.
65. Lau,P.W., Potter,C.S., Carragher,B. and MacRae,I.J. (2009) Structure of the human Dicer-TRBP complex by electron microscopy. *Structure*, **17**, 1326–1332.
66. Wang,H.W., Noland,C., Siridechadilok,B., Taylor,D.W., Ma,E., Felderer,K., Doudna,J.A. and Nogales,E. (2009) Structural insights into RNA processing by the human RISC-loading complex. *Nat. Struct. Mol. Biol.*, **16**, 1148–1153.
67. Kawahara,Y., Zinshteyn,B., Chendrimada,T.P., Shiekhattar,R. and Nishikura,K. (2007) RNA editing of the microRNA-151 precursor blocks cleavage by the Dicer-TRBP complex. *EMBO Reports*, **8**, 763–769.
68. Provost,P., Dishart,D., Doucet,J., Frendewey,D., Samuelsson,B. and Radmark,O. (2002) Ribonuclease activity and RNA binding of recombinant human Dicer. *EMBO J.*, **21**, 5864–5874.